

# Stability of current filaments in a bistable semiconductor system with global coupling

A. Alekseev

*Institute for Theoretical Physics, Uppsala University, Box 803, S-75108 Uppsala, Sweden*

S. Bose, P. Rodin,\* and E. Schöll

*Institut für Theoretische Physik, Technische Universität Berlin, Hardenbergstrasse 36, D-10623, Berlin, Germany*

(Received 1 October 1997)

We study the stability of steady current filaments in a bistable semiconductor system in the presence of global coupling given by an external circuit. The system is described by a reaction-diffusion model on a two-dimensional spatial domain with Neumann boundary conditions. We prove generally for the voltage-driven regime that in a convex domain any filament has at least one unstable linear eigenmode. Introducing a global coupling may either eliminate the unstable mode with the largest increment or induce oscillatory instabilities. Filaments with negative differential conductance can be stabilized by strong global coupling. Stabilization of filaments with positive differential conductance can be achieved only by an active external circuit with negative resistance and capacitance. We present analytical arguments and numerical simulations suggesting that the boundary of the domain always attracts current filaments. Our numerical results also show that seed inhomogeneities may pin current filaments in the center of sufficiently large domains. The competition between the attractive boundary and pinning by seed inhomogeneities is studied numerically. [S1063-651X(98)06303-X]

PACS number(s): 05.70.Ln, 72.20.Ht

## I. INTRODUCTION

Current filamentation in semiconductor systems with bistable current-voltage characteristics represents one of the simplest nontrivial examples of pattern formation in active spatially extended media [1]. Current filaments are characterized by a current density profile, which varies in the plane perpendicular to the current flow reflecting spatial coexistence of the two stable phases. According to the concept of pattern formation in activator-inhibitor systems [2–7] current filamentation may occur due to the competition between an internal mechanism of activation, which provides negative differential conductivity (NDC) of the semiconductor element [8], and an external mechanism of inhibition given by the constraint related to the external circuit. The theoretical description of stationary current filaments, originally developed for semiconductors with an electron overheating instability [9–11], has been later advanced for other semiconductor systems exhibiting *s*-shaped negative differential conductivity (SNDC) [12–21]. It was also discovered that current filaments can exhibit temporal instabilities that lead to traveling or rocking filaments [22], and small-amplitude or relaxation-type oscillations, known as breathing [23,24] and spiking of a current filament [25–27], respectively. A well-known approach is to treat the problem in terms of a one-dimensional reaction-diffusion equation, which results from the reduction of two-dimensional transport models, and an integrodifferential equation corresponding to a global constraint given by the external circuit (e.g., [11,25,28]). Since the model equation takes into account only one transversal degree of freedom for the current density distribution such a

theory is adequate only for samples with effectively one-dimensional striplike geometries where the longitudinal coordinate parallel to the current flow has been eliminated, and the second transversal dimension is so short that spatial instabilities cannot develop. The description of real three-dimensional samples requires models on two-dimensional (transversal) spatial domains. Up to now most studies of two-dimensional models have either assumed axial symmetry of the current distribution [15,16,23,24], or have considered the longitudinal and one transversal coordinate only [29,30], which is appropriate for thin semiconductor films. Recent numerical simulations of filament dynamics on quadratic domains [31] have been performed for an activator-inhibitor model, which takes into account both local inhibition processes inside the semiconductor structure and global inhibition due to the external circuit.

The purpose of this paper is to develop analytical and numerical results for bulk samples where both transversal dimensions are of comparable size. We concentrate on the stability of steady current filaments in bistable semiconductor systems that do not experience local internal inhibition and present a general approach for arbitrary convex two-dimensional spatial domains with proper account taken for global coupling. A typical sample geometry is shown in Fig. 1. An external circuit with load resistor  $R$  and capacitor  $C$  is attached to the top ( $K$ ) and bottom ( $A$ ) contacts of the sample.

We assume that the internal state of the semiconductor system can be characterized by a single spatially distributed parameter  $a(x, y, t)$ , which corresponds to the internal degree of freedom relevant to the bistability. The physical meaning of this parameter might be electron temperature [9,10], concentration of excess carriers [16], bias of one of the *pn* junctions in a thyristor [12,19], interface charge density of a heterostructure hot electron diode [25], etc., depending upon the

\*On leave from A. F. Ioffe Physicotechnical Institute, Russian Academy of Science, 194021 St. Petersburg, Russia.

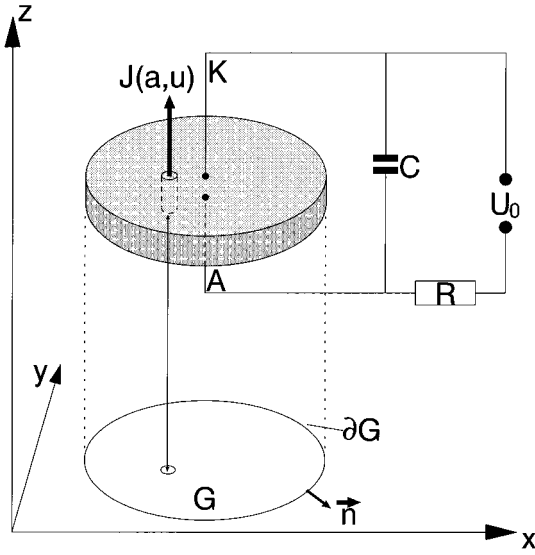


FIG. 1. Schematic sketch of the semiconductor structure (shaded) and the external circuit attached to its cathode ( $K$ ) and anode ( $A$ ) contacts. The direction of current flow  $J(a,u)$  and a cylindrical current filament are schematically indicated. The projection onto the  $(x,y)$  plane shows the two-dimensional domain  $G$  under study;  $\vec{n}$  denotes the normal vector at the boundary  $\partial G$ .

specific transport mechanism. The variable  $a(x,y,t)$  and the voltage  $u(t)$  across the sample determine the current density  $J(a,u)$  in a cross section of the device. For various semiconductor systems [9–13,17,19,22,25,32,33] the spatiotemporal dynamics of  $a(x,y,t)$  is described by a reaction-diffusion equation of the type

$$\tau_a \frac{\partial a(x,y,t)}{\partial t} = l_a^2 \Delta a(x,y,t) + f(a(x,y,t), u(t)). \quad (1)$$

Here  $\tau_a$  and  $l_a$  characterize the relaxation time and transversal diffusion length, respectively. The local kinetic function  $f(a,u)$  is a nonmonotonic function of  $a$ , which, for fixed  $u$  in a certain range, has three zeroes corresponding to high-conductivity, low-conductivity, and negative differential conductivity (NDC) states [Fig. 2(a)]. Since  $\partial f/\partial a > 0$  for values of  $u$  in the NDC range, the variable  $a$  may be regarded as an activator. The functions  $f(a,u)$  and  $J(a,u)$  contain all necessary information about vertical transport along the  $z$  direction in the structure shown in Fig. 1. Generally, in the steady state, the local dependence  $a(u)$  is cal-

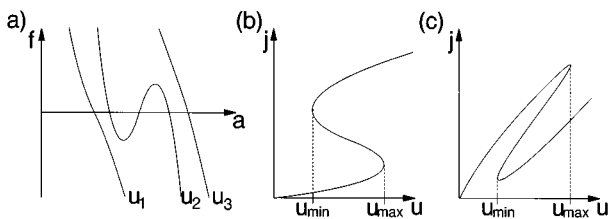


FIG. 2. (a) Local kinetic function  $f(a,u)$  for different values of  $u$  ( $u_1 < u_{\min}$ ,  $u_{\min} < u_2 < u_{\max}$ ,  $u_3 > u_{\max}$ ). (b),(c)  $s$ - and  $z$ -shaped local current density vs voltage characteristics  $j(u)$ , respectively (schematic).

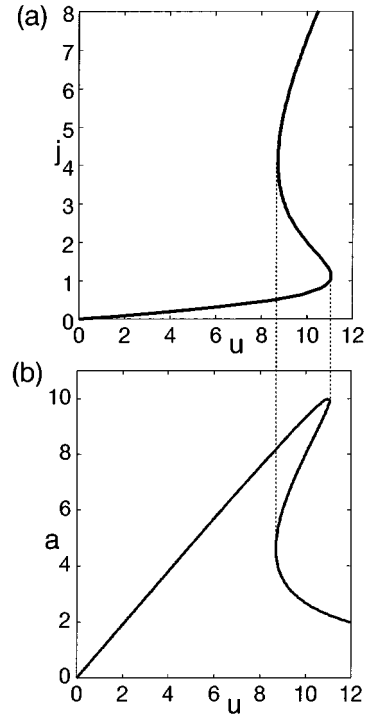


FIG. 3. (a) Local current density-voltage characteristic  $j(u)$  and (b) null-isocline  $a(u)$  given by  $f(a,u)=0$  for the model functions Eq. (2) with  $T=0.05$ .

culated from the null-isocline  $f(a,u)=0$  and inserted into  $J(a,u)$  to find the local current density-voltage characteristic  $j(u) \equiv J(a(u), u)$  which can be  $s$ -shaped [Fig. 2(b)] or  $z$ -shaped [Fig. 2(c)] (see [33] for a discussion of the general case and some examples). However, a particular type of non-linearity is not crucial for the present analysis. In our analytical considerations we will not specify the dependencies of  $f(a,u)$ ,  $J(a,u)$ , and will only assume the condition  $\partial J/\partial u > 0$ . In our numerical examples we will use the following model functions, which were originally derived for the heterostructure hot-electron diode (HHED) but were shown to hold more generally for layered semiconductor structures [25]:

$$f(a,u) = \frac{u-a}{(u-a)^2+1} - Ta, \quad J(a,u) = u-a. \quad (2)$$

These functions result in a  $z$ -shaped  $a(u)$  dependence and an  $s$ -shaped  $j(u)$  dependence (Fig. 3). Note that dimensionless variables are used here.

The distribution  $a(x,y,t)$  has to satisfy Neumann boundary conditions corresponding to a passive boundary with no flux:

$$\left. \frac{\partial a(x,y,t)}{\partial n} \right|_{\partial G} = 0. \quad (3)$$

Here  $\partial/\partial n$  is the normal derivative at the boundary  $\partial G$  of the domain  $G$ .

The temporal dynamics of the voltage  $u(t)$  is described by Kirchhoff's equation for the external circuit:

$$\tau_u(u) \frac{du(t)}{dt} = g(a, u), \quad g(a, u) \equiv U_0 - u(t) - RS \langle J(a, u) \rangle,$$

$$\tau_u(u) \equiv RC(u), \quad C(u) \equiv C_{\text{ext}}(u) + C_{\text{int}}(u), \quad (4)$$

where  $U_0$  is the applied bias voltage,  $R$  is the load resistance,  $C_{\text{int}}$  is the internal differential capacitance of the sample,  $C_{\text{ext}}$  is the differential capacitance of the external circuit,  $S$  is the cross section of the device, and the angular brackets denote the spatial average over the domain  $G$ . Since generally the derivatives  $\partial g/\partial a$  and  $\partial f/\partial u$  have different signs in the NDC range, the variable  $u$  acts as inhibitor. (Specifically,  $\partial g/\partial a > 0$ ,  $\partial f/\partial u < 0$  hold for the dependencies (2),  $\partial g/\partial a < 0$ ,  $\partial f/\partial u > 0$  hold for models of overheating instabilities [9–11] and multilayered structures [12–14, 19, 36].) Equation (4) represents a global constraint that is imposed on the dynamics of  $a(x, y, t)$  and provides global coupling between distant parts of the cross section.

Linearization of the equations (1), (4) in the vicinity of a stationary solution  $a_0(x, y)$ ,  $u_0$  with respect to the perturbation  $e^{\zeta t} \delta a(x, y) = [a(x, y, t) - a_0(x, y)]$ ,  $e^{\zeta t} \delta u = [u(t) - u_0]$  with  $\partial \delta a(x, y)/\partial n|_{\partial G} = 0$  yields

$$\tau_a \zeta \delta a = \hat{H}_N \delta a + \frac{\partial f}{\partial u} \delta u, \quad \hat{H}_N = l_a^2 \Delta + \Phi(x, y),$$

$$\Phi(x, y) \equiv \frac{\partial f}{\partial a} \Big|_{a_0, u_0}, \quad (5)$$

$$\tau_u \zeta \delta u = - \left( 1 + RS \left\langle \frac{\partial J}{\partial u} \right\rangle \right) \delta u - RS \left\langle \frac{\partial J}{\partial a} \delta a \right\rangle, \quad \tau_u = \tau_u(u_0). \quad (6)$$

Here and further on the characteristic time  $\tau_u$  and partial derivatives of  $f$  and  $J$  are computed at the steady state  $a_0, u_0$ . The stationary solution is stable if  $\text{Re} \zeta < 0$  for all eigenvalues  $\zeta$ .

The self-adjoint operator  $\hat{H}_N$  acts on the space of functions with Neumann boundary conditions. Its eigenfunctions  $\Psi_i$  and eigenvalues  $\lambda_i$  correspond to eigenmodes and eigenvalues of the voltage-driven system ( $R = C = 0$ ): according to Eqs. (5) and (6)  $\zeta = \lambda/\tau_a$  for  $\delta u = 0$ . So the voltage-driven system is stable if all  $\lambda_i < 0$ . In the presence of the global constraint Eq. (6) mixes the eigenmodes  $\Psi_i$ . In this case we should analyze both equations (5) and (6) simultaneously, but the knowledge of the spectrum  $\{\lambda_i\}$  remains the key to the stability problem.

Our aim is to establish a link between stability and such general features of a filamentary state as the location of the extremum and the sign of the differential conductivity. [Whereas in a one-dimensional theory [15, 16] the complete classification of  $a_0(x, y)$  follows from the phase-portrait analysis of Eq. (1), in the two-dimensional case such a classification is not available even for domains of simple shape.] The paper is organized as follows. In Sec. II we study the spectrum  $\lambda_i$  of the operator  $\hat{H}_N$  related to the spatial domain  $G$  of arbitrary shape. In Sec. III we concentrate on the effect of the global coupling on filament stability and establish a connection between the number of unstable modes [ $\text{Re}(\zeta) > 0$ ] of the complete stability problem and the number of

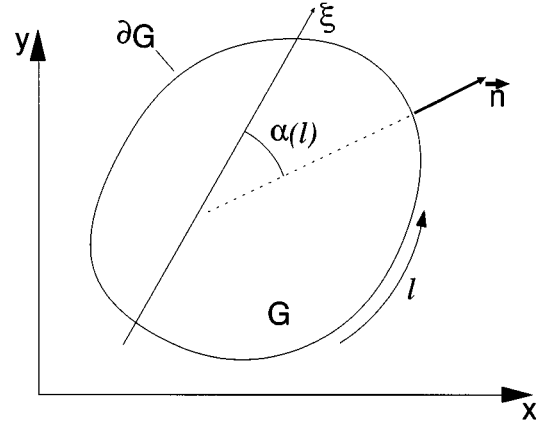


FIG. 4. Domain  $G$  (schematic): The direction  $\xi$  corresponds to the translation mode  $\vartheta_G$ ,  $l$  is a coordinate along the boundary  $\partial G$ ,  $\vec{n}$  is the external normal to the boundary.

positive eigenvalues  $\lambda_i$  corresponding to the voltage-driven system. In Sec. IV we use the results of Secs. II and III to formulate some general criteria of filament stability. Here we also present the results of numerical simulations and discuss the effect of embedded inhomogeneities of the semiconductor structure on filament stability.

## II. EIGENVALUES OF VOLTAGE-DRIVEN SYSTEM

The eigenvalues of the operator  $\hat{H}_N$  may be ordered by decreasing size,  $\lambda_1 > \lambda_2 > \dots$ . In this section we study the sign of the first two eigenvalues  $\lambda_1, \lambda_2$ . The first eigenmode  $\Psi_1$  is strictly positive inside the domain  $G$  and hence represents the switching mode, which leads to expansion or shrinking of a filament. The interpretation of the second eigenmode  $\Psi_2$  depends on the particular solution  $a_0(x, y)$ . For filaments in the interior of the domain it corresponds to the shift of a filament along a certain direction [16].

To analyze the spectrum of the operator  $\hat{H}_N$  let us introduce the translation modes (these modes are also known as Goldstone modes [16])

$$\vartheta_G(x, y) \equiv \frac{da_0(x, y)}{d\xi}, \quad (7)$$

where  $d/d\xi$  is the derivative along the direction  $\xi$  on the  $(x, y)$  plane (Fig. 4). Boundary conditions for  $\vartheta_G(x, y)$  can be obtained by direct calculation taking into account that  $a_0(x, y)$  satisfies Neumann boundary conditions on  $\partial G$ :

$$\vartheta_G(l) = \frac{\partial a_0}{\partial l} \sin \alpha(l),$$

$$\frac{\partial \vartheta_G(l)}{\partial n} = \frac{1}{R(l)} \frac{\partial a_0}{\partial l} \sin \alpha(l) + \frac{\partial^2 a_0}{\partial n^2} \cos \alpha(l). \quad (8)$$

Here  $l$  is a coordinate along the boundary,  $\alpha(l)$  is an angle between the direction  $\xi$  and the external normal  $\vec{n}$ ,  $R(l)$  is the radius of curvature of the domain boundary  $\partial G$ . The translation modes correspond to zero eigenvalues of the op-

erator  $\hat{H}_{g(l)}$ , which is defined by the same expression as  $\hat{H}_N$  [see Eq. (5)] but acts on the space of functions with linear boundary conditions

$$\left( g(l)\Psi(x,y) + \frac{\partial\Psi(x,y)}{\partial n} \right) \Big|_{\partial G} = 0. \quad (9)$$

In particular, the function  $g(l)$  can be chosen in such a way that  $\vartheta_G$  satisfies Eq. (9) (note that different directions  $\xi$  correspond to different operators  $\hat{H}_{g(l)}$ ):

$$g(l) = -\frac{1}{R(l)} - \left( \frac{\partial^2 a_0}{\partial n^2} \right) \left( \frac{\partial a_0}{\partial l} \right)^{-1} \cot\alpha(l). \quad (10)$$

The quadratic form  $\tilde{H}_{g(l)}$  of the operator  $\hat{H}_{g(l)}$  given by the scalar product  $\langle \Psi \hat{H}_{g(l)} \Psi \rangle$  can be represented as

$$\begin{aligned} \tilde{H}_{g(l)}(\Psi) &\equiv \int_G \Psi \hat{H}_{g(l)} \Psi dx dy \\ &= -l_a^2 \int_{\partial G} g(l) \Psi^2 dl + \int_G [-l_a^2 (\nabla \Psi)^2 \\ &\quad + \Phi(x,y) \Psi^2] dx dy. \end{aligned} \quad (11)$$

In order to determine the sign of the first eigenvalue of the operator  $\hat{H}_N$  we apply the variational principle [35], which states that eigenfunctions of  $\hat{H}_N$  are extrema of its quadratic form

$$\tilde{H}_N(\Psi) = \int_G [-l_a^2 (\nabla \Psi)^2 + \Phi(x,y) \Psi^2] dx dy. \quad (12)$$

The eigenfunction  $\Psi_1$  corresponding to the largest eigenvalue of  $\hat{H}_N$  provides the maximum of  $\tilde{H}_N$ .

Since the variation of the quadratic form (11) includes the boundary term  $\int_{\partial G} (\partial\Psi/\partial n) \delta\Psi dl$ , which vanishes only if  $\partial\Psi/\partial n = 0$ ,  $\tilde{H}_N(\Psi)$  automatically imposes Neumann boundary conditions on its extrema. Therefore, if we present any function  $\Psi$  for which  $\tilde{H}_N(\Psi) > 0$ , then the operator  $\hat{H}_N$  has at least one positive eigenvalue. Since  $\vartheta_G$  is a zero mode of  $\hat{H}_{g(l)}$  [ $\tilde{H}_{g(l)}(\vartheta_G) = 0$ ] and on account of Eqs. (11),(12), we obtain

$$\tilde{H}_N(\vartheta_G) = l_a^2 \int_{\partial G} \vartheta_G \frac{\partial \vartheta_G}{\partial n} dl. \quad (13)$$

Substituting Eq. (8) into Eq. (13) leads to

$$\begin{aligned} \tilde{H}_N(\vartheta_G) &= l_a^2 \int_{\partial G} \left[ \frac{1}{R} \left( \frac{\partial a_0}{\partial l} \right)^2 \sin^2 \alpha(l) \right. \\ &\quad \left. + \frac{1}{2} \frac{\partial a_0}{\partial l} \frac{\partial^2 a_0}{\partial n^2} \sin 2\alpha(l) \right] dl. \end{aligned} \quad (14)$$

Now let us choose two translation modes  $\vartheta_G^1$  and  $\vartheta_G^2$  corresponding to orthogonal directions. According to Eq. (14) the sum of their quadratic forms can be represented as

$$\Sigma \equiv \tilde{H}_N(\vartheta_G^1) + \tilde{H}_N(\vartheta_G^2) = l_a^2 \int_{\partial G} \frac{1}{R(l)} \left( \frac{\partial a_0}{\partial l} \right)^2 dl. \quad (15)$$

For any convex domain [ $R(l) > 0$ ] we obtain  $\Sigma \geq 0$ . Let us prove that from  $\Sigma \geq 0$  follows  $\lambda_1 > 0$ . Indeed, in the case  $\Sigma > 0$  at least one of the quadratic forms  $\tilde{H}_N(\vartheta_G^1), \tilde{H}_N(\vartheta_G^2)$  is positive. Then from the variational principle it follows that  $\hat{H}_N$  has at least one positive eigenvalue. The equalities  $\Sigma = 0$  and  $\lambda_1 = 0$  cannot occur simultaneously because in this case either  $\vartheta_G^1 = 0, \vartheta_G^2 = 0$  or  $\vartheta_G^1 = \Psi_1, \vartheta_G^2 = 0$ . In the first case  $a_0 = \text{const}$ , in the second case  $a_0$  corresponds to a plane current layer and its translation mode can never coincide with  $\Psi_1$  due to the boundary conditions. Therefore again  $\lambda_1 > 0$ . Thus, for the operator  $\hat{H}_N$  defined on any convex domain  $\lambda_1 > 0$  and the ground state eigenfunction  $\Psi_1$  corresponds to an unstable mode. (A similar but more cumbersome proof of this fact for  $n$ -dimensional domains has been presented in [34] in application to dissipative structures in ecological systems.)

In order to determine the sign of the second eigenvalue we should establish some relation between  $\hat{H}_N$  and  $\hat{H}_{g(l)}$  and use the fact that the operator  $\hat{H}_{g(l)}$  has a zero eigenmode  $\vartheta_G$ . From the theory of operators [35] it follows that  $\hat{H}_N > \hat{H}_{g(l)}$  (i.e.,  $\lambda_i > \lambda_i^{g(l)}$  for any  $i$ ) if  $\tilde{H}_N > \tilde{H}_{g(l)}$  or if  $\tilde{H}_N = \tilde{H}_{g(l)}$  and the domain  $D(\tilde{H}_N)$  of  $\tilde{H}_N$  [ $D(\tilde{H}_N)$  is a set of functions on which  $\tilde{H}_N$  is defined] includes the domain  $D(\tilde{H}_{g(l)})$  for  $\tilde{H}_{g(l)}$ :  $D(\tilde{H}_N) \supset D(\tilde{H}_{g(l)})$ . The difference between the quadratic forms  $\tilde{H}_N$  (12) and  $\tilde{H}_{g(l)}$  (11)

$$\tilde{H}_N(\Psi) - \tilde{H}_{g(l)}(\Psi) = l_a^2 \int_{\partial G} g(l) \Psi^2 dl \quad (16)$$

is positive when  $g(l) > 0$ . However, the condition  $g(l) > 0$  is violated for any solution  $a_0$  that varies along the boundary  $\partial G$ . Indeed, at the boundary point where  $\xi$  and  $n$  are parallel  $\cot\alpha(l)$  changes sign whereas  $\partial^2 a_0 / \partial n^2$  in general does not. Therefore  $\hat{H}_N$  and  $\hat{H}_{g(l)}$  cannot be compared if  $a_0(l) \neq \text{const}$ . When  $a_0(l) = \text{const}$  Eq. (10) implies that all translation modes satisfy the Dirichlet boundary conditions [ $g(l) = \infty$ ]. Then the operator  $\hat{H}_{g(l)}$  is a Dirichlet one:  $\hat{H}_{g(l)} = \hat{H}_D$ . In this case  $\tilde{H}_N = \tilde{H}_D$ . Since  $\tilde{H}_N$  can be considered on functions with arbitrary boundary condition the domain of  $\tilde{H}_N$  contains the domain of  $\tilde{H}_D$ . Thus,  $\hat{H}_N > \hat{H}_D$ .

Any inhomogeneous state  $a_0$  that satisfies the condition  $a_0(l) = \text{const}$  has an extremum inside the domain  $G$  and its translation mode  $\vartheta_G$  always has zeros. As the ground state eigenfunction of the operator  $\hat{H}_D$  is strictly positive, the eigenvalue  $\lambda_i^D = 0$  corresponds to  $i \geq 2$ . Taking into account  $\hat{H}_N > \hat{H}_D$  we conclude that  $\lambda_2 > 0$ .

Thus we have established that for any steady inhomogeneous state  $a_0(x,y)$  on a convex domain  $\lambda_1 > 0$  holds, and that for any steady state which satisfies the condition  $a_0(x,y)|_{\partial G} = \text{const}$  on an arbitrary domain  $\lambda_1 > 0, \lambda_2 > 0$  hold. Note that the condition of convexity of the domain and the condition  $a_0(x,y)|_{\partial G} = \text{const}$  are sufficient but not necessary conditions for  $\lambda_1 > 0$  and  $\lambda_1 > 0, \lambda_2 > 0$ , respectively.

Since for one-dimensional domains the translation mode  $\vartheta_G$  always satisfies Dirichlet boundary conditions, it also follows from our analysis that  $\lambda_1 > 0$  for any one-dimensional distribution  $a_0(x)$  and  $\lambda_1 > 0, \lambda_2 > 0$  for nonmonotonic  $a_0(x)$ .

### III. EFFECT OF THE GLOBAL CONSTRAINT ON FILAMENT STABILITY

In this section we establish the relation between the number of unstable modes ( $\text{Re}\zeta > 0$ ) in the presence of a global constraint and the number of positive eigenvalues  $\lambda_i$  corresponding to the voltage-driven regime. We advance the approach originally suggested for semiconductors with an electron overheating instability [11]. Stability of current filaments in controllable bistable systems with two external global constraints have recently been studied in [36].

Let us expand the eigenmode  $\delta a(x, y)$  in the basis of the eigenfunctions  $\Psi_i$  of the operator  $\hat{H}_N$ :

$$\delta a(x, y) = \sum_m \langle \delta a \cdot \Psi_m \rangle \Psi_m. \quad (17)$$

From Eq. (5) we obtain the coefficients of this expansion

$$\delta a(x, y) = \sum_m \frac{\langle \partial f / \partial u \Psi_m \rangle}{\tau_a \zeta - \lambda_m} \delta u \Psi_m(x, y). \quad (18)$$

Substituting into Eq. (6) leads to the characteristic equation

$$\begin{aligned} F(\zeta) &= F_0(\zeta) + F_1(\zeta) = 0, \\ F_0(\zeta) &= 1 + RS \left\langle \frac{\partial J}{\partial u} \right\rangle + RS \sum_m \frac{\langle \partial f / \partial u \Psi_m \rangle \langle \partial J / \partial a \Psi_m \rangle}{\tau_a \zeta - \lambda_m}, \\ F_1(\zeta) &= \tau_u \zeta, \end{aligned} \quad (19)$$

which determines the complex eigenvalues  $\zeta$  of the linearized system (5),(6). We separate the two parts  $F_0(\zeta)$  and  $F_1(\zeta)$  such that the characteristic time of the inhibitor  $\tau_u$  enters only  $F_1(\zeta)$ . Note that the ground state eigenfunction  $\Psi_1$  has no zeroes whereas the  $\Psi_i$  oscillate in space for  $i > 1$ . Therefore the first term dominates the others in the sum in the last term of  $F_0(\zeta)$ .

Taking into account that  $\zeta=0$  for variations  $\delta a(x, y)$  along the steady current-voltage characteristic and applying Eq. (18), we can represent the differential conductance of the inhomogeneous state

$$\sigma_d \equiv S \frac{d\langle J(a, u) \rangle}{du} = S \left( \left\langle \frac{\partial J}{\partial u} \right\rangle + \left\langle \frac{\partial J}{\partial a} \frac{\delta a}{\delta u} \right\rangle \right) \quad (20)$$

as

$$\sigma_d = \sigma_u - S \sum_m \frac{\langle \partial f / \partial u \Psi_m \rangle \langle \partial J / \partial a \Psi_m \rangle}{\lambda_m}, \quad \sigma_u \equiv S \left\langle \frac{\partial J}{\partial u} \right\rangle, \quad (21)$$

where  $\sigma_u$  denotes the differential conductance for fixed internal parameter  $a(x)$ . Note that  $\sigma_u > 0$ .

Zeroes of the characteristic function  $F(\zeta)$  are complex eigenvalues of the stability problem (5),(6) and its poles are

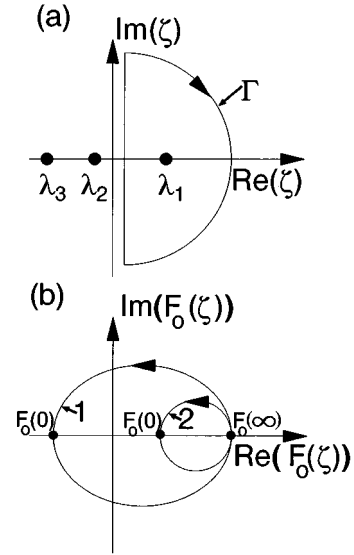


FIG. 5. Stability analysis using the characteristic equation. (a) Contour  $\Gamma$  in the complex  $\zeta$  plane encircles the right half-plane, which contains eigenvalues  $\zeta$  with positive real parts.  $\lambda_1, \lambda_2, \lambda_3$  are poles corresponding to the eigenvalues for the voltage-driven case. (b) Mapping  $F_0(\Gamma)$  of the contour  $\Gamma$  corresponding to the case of fast inhibition  $\tau_a \gg \tau_u$ . Contours 1 and 2 correspond to the case of Eqs. (25) and (26), respectively.

eigenvalues  $\lambda_i$  of the operator  $\hat{H}_N$ . The number of poles  $P$  and the number of zeroes  $N$  located inside any closed contour  $\Gamma$  in the complex  $\zeta$  plane are related by the argument principle:

$$N = P + \frac{1}{2\pi} \Delta \text{Arg} F(\zeta), \quad (22)$$

where  $\Delta \text{Arg} F(\zeta)$  is the variation of the argument of  $F(\zeta)$  when  $\zeta$  varies along the contour  $\Gamma$  [37]. As unstable modes correspond to  $\text{Re}\zeta > 0$  we choose the contour  $\Gamma$  encircling the right half-plane [Fig. 5(a)] in the clockwise direction. The variation  $\Delta \text{Arg} F(\zeta)$  depends on how many times and in which direction the contour  $F(\Gamma)$  turns around the origin. In the case of anticlockwise rotation the number of unstable eigenmodes is less than the number of positive eigenvalues  $\lambda_i$  by the number of turns, in the case of clockwise rotation it is larger by the same number.  $N = P$  holds if  $F(\Gamma)$  does not encircle the origin.

First, let us consider the case of fast inhibition  $\tau_u \ll \tau_a$  when temporal instabilities are damped out in favor of spatial ones. Then we neglect the term  $F_1$  in the characteristic equation. In this case

$$F(0) = 1 + R\sigma_d, \quad F(\infty) = 1 + R\sigma_u, \quad (23)$$

Therefore the contour  $F(\Gamma)$  encircles the origin once if  $\text{sgn}\{F(\infty)\} = -\text{sgn}\{F(0)\}$  and the direction of rotation of  $F(\Gamma)$  is anticlockwise [Fig. 5(b)]. This leads to the following stability criterion:

$$-\sigma_u < R^{-1} < -\sigma_d. \quad (24)$$

When this criterion is met the global constraint reduces the number of unstable modes related to the operator  $\hat{H}_N$  by one

$$N = P - 1, \quad (25)$$

otherwise

$$N = P. \quad (26)$$

In the last case the global constraint has no impact on stability, and the system behavior is similar to the voltage-driven regime. In what follows we refer to the cases (25) and (26) as to regimes of strong and weak global coupling, respectively.

Therefore in the regime of weak coupling the system is stable if all eigenvalues  $\lambda_i$  of the operator  $\hat{H}_N$  are negative, whereas in the case of strong coupling the system remains stable even if the first eigenvalue  $\lambda_1$  is positive. For filamentary states with NDC ( $\sigma_d < 0$ ) the criterion (24) can be fulfilled with a linear passive external circuit and it takes the conventional form  $R > |\sigma_d|^{-1}$ . This occurs for a heavily loaded external circuit and corresponds to the regime of strong global coupling. For filamentary states with positive differential conductance (PDC) the criterion (24) demands  $R < 0$ . A negative external load resistance can be realized by active circuits: An experimental setup exhibiting an absolute negative resistance  $R < 0$  and a negative (both absolute and differential) capacitance  $C < 0$  has been reported recently [38].

Since for  $R < 0$  an instability can also be induced by the negative load itself, in a valid stability analysis one should then properly take into account also the action of the temporal degree of freedom related to the external circuit, i.e., one should treat the case  $\tau_u \neq 0$ . As we have already shown that filamentary states with two or more positive eigenvalues  $\lambda_1 > 0, \lambda_2 > 0$  remain unstable if a global constraint is imposed, it is sufficient to consider the case  $\lambda_1 > 0, \lambda_2 < 0$ . Leaving only the first term corresponding to  $\lambda_1$  in the sum in Eq. (19), we write the characteristic equation in the form

$$C\tau_a\zeta^2 + [\tau_a(R^{-1} + \sigma_u) - C\lambda_1]\zeta - \lambda_1(R^{-1} + \sigma_d) = 0. \quad (27)$$

For  $\lambda_1 > 0$  this equation leads to a modified version of the stability criterion (24) [taking  $F_1(\zeta)$  into account one arrives at similar qualitative conclusions by applying complex-plane analysis],

$$-\sigma_u + \frac{C\lambda_1}{\tau_a} < R^{-1} < -\sigma_d \quad \text{if } C > 0, \quad (28)$$

$$-\sigma_d < R^{-1} < -\sigma_u + \frac{C\lambda_1}{\tau_a} \quad \text{if } C < 0. \quad (29)$$

For the cases  $C > 0$  (28) and  $C < 0$  (29) a Hopf bifurcation, where a pair of complex conjugate eigenvalues  $\zeta$  crosses the imaginary axis, occurs at the lower and upper bound, respectively. This condition shows that oscillatory instabilities are possible if the total capacitance  $|C|$  exceeds a critical value  $C_{\text{crit}}$ .

The criteria (28),(29) allow us to understand how to stabilize the filamentary states with PDC. Indeed, for  $\sigma_d > 0$  the condition (28) can be met only if  $\sigma_d < \sigma_u$  (and  $R < 0$ ). Since

the main contribution to the differential conductance of a filamentary state usually comes from the shift of the filament wall [the second term in Eq. (21)], in most situations  $|\sigma_d| > |\sigma_u|$ . Therefore the condition (28) cannot be met, and filaments with PDC can be stable only in the case  $R < 0, C > 0$  described by Eq. (29). The requirement of a negative capacitance has a simple qualitative explanation: for  $R < 0, C > 0$  the characteristic time  $\tau_u = RC$  becomes negative, which indicates an instability induced by the external circuit.

Since we have not specified the type of spatial distribution  $a_o(x,y)$  under study, the analysis performed in this section is also valid for homogeneous states. For instance, for uniform states on the middle branch of an *s*- or *z*-shaped characteristic  $\lambda_1 = \partial f / \partial a > 0$ ,  $\lambda_2 \approx \partial f / \partial a - (\pi l_a / L)^2$ , where  $L$  is the largest transverse dimension of the domain  $G$ . For the case of a small domain  $\lambda_1 > 0, \lambda_2 < 0$  our analysis leads to the results obtained for space-clamped elements in [33]. For a sufficiently large domain the second eigenvalue is also positive ( $\lambda_1 > 0, \lambda_2 > 0$ ) and a homogeneous state cannot be stabilized by a global constraint.

An oscillatory instability of current filaments might result in either homogeneous oscillations or breathing [23] or spiking filaments [26]. It is known from one-dimensional analyses that hysteresis between steady current filaments and the spiking mode takes place for the major part of the parameter space [27]. Therefore, if a steady filament is already unstable, the spiking mode is unlikely to appear. As for inhomogeneous states  $\lambda_1 < \partial f / \partial a$ , according to Eq. (28) a filamentary state is more stable with respect to oscillatory instabilities than homogeneous states with NDC. For this reason in the simplest case of *s*-type NDC a limit cycle corresponding to homogeneous oscillations already exists for system parameters at which a Hopf bifurcation of the filamentary state occurs, and hence homogeneous self-generated oscillations rather than breathing filaments emerge as the most probable result of the instability. Obviously, the global behavior after the bifurcation also essentially depends on the form and position of the null-isoclines  $f(a,u) = 0$  and  $g(a,u) = 0$  [or the local current density-voltage characteristic and the load line, which give an equivalent representation in the  $(j,u)$  plane] and, in particular, on the number of their intersections. This is especially important for systems with *z*-shaped current-voltage characteristics where usually several points of intersection exist.

#### IV. CURRENT FILAMENTS ON TWO-DIMENSIONAL DOMAINS

General results of the stability analysis performed in Secs. II and III are summarized in Table I. In the regime of weak global coupling (weakly loaded external circuit) any stationary filamentary state  $a_o(x,y)$  on a convex domain is unstable. The switching mode dominates the growth of perturbations. This leads either to expansion or shrinking of the current filament. In the case  $R > 0$  the stability criterion (28) is never met for filaments with PDC, and therefore the presence of a global constraint and NDC of the filamentary state are necessary conditions of stability. Stability of a filament with PDC requires a negative external load  $R < 0$  in the case  $\sigma_d < \sigma_u$  (28), and a negative external load  $R < 0$  together

TABLE I. Result of the stability analysis of current filaments.

Type of global coupling	Type of steady current density distribution	
	Arbitrary nonuniform distribution, convex domain $G$	Distribution with an extremum inside $G$ , $a_0 _{\partial G} = \text{const}$ , arbitrary domain $G$
No coupling: (voltage-driven regime) $R=0$	Unstable: $\lambda_1 > 0$ ; $\text{sign} \lambda_2$ undetermined	Unstable: $\lambda_1 > 0, \lambda_2 > 0$
Weak global coupling: $R^{-1} \notin \left[ -\sigma_u + \frac{C\lambda_1}{\tau_a}; -\sigma_d \right]$ for $C > 0$	Unstable: at least one unstable mode	Unstable: at least two unstable modes
$R^{-1} \notin \left[ -\sigma_d; -\sigma_u + \frac{C\lambda_1}{\tau_a} \right]$ for $C < 0$		
Strong global coupling: $R^{-1} \in \left[ -\sigma_u + \frac{C\lambda_1}{\tau_a}; -\sigma_d \right]$ for $C > 0$	Stable if and only if $\lambda_2 < 0$	Always unstable against translation mode
$R^{-1} \in \left[ -\sigma_d; -\sigma_u + \frac{C\lambda_1}{\tau_a} \right]$ for $C < 0$		

with negative differential capacitance  $C < 0$  in the case  $\sigma_d > \sigma_u$  (29).

For domains that are not convex the sign of  $\lambda_1$  is unknown in general. It has been shown [34] that  $\lambda_1 < 0$  holds for a dumbbell-shaped domain, which represents two circular domains connected by a sufficiently narrow crosspiece. This domain corresponds to two weakly coupled SNDC elements. As  $\lambda_1 < 0$ , coexistence of high-conductivity and low-conductivity states is possible in such a system even in the voltage-driven regime.

In the case of strong global coupling and NDC of the filamentary state the number of unstable modes  $\lambda_i > 0$  associated with the voltage-driven system is reduced by one. Therefore the filament stability depends on the sign of the second eigenvalue  $\lambda_2$ . We have proved that  $\lambda_2 > 0$  holds for any distribution  $a_0(x, y)$  that has a maximum inside the domain and does not vary along its boundary ( $a_0|_{\partial G} = \text{const}$ ). Here we do not require convexity of the domain. According to this conclusion a filament located in the interior of the domain is unstable and is attracted by the boundary of the domain.

Let us illustrate this statement by the example of radially symmetrical filaments in circular domains. Assuming radial symmetry, we write Eq. (1) in the steady state in polar coordinates  $(r, \phi)$  as in [15,16]:

$$l_a^2 \left( \frac{\partial^2 a}{\partial r^2} + \frac{1}{r} \frac{\partial a}{\partial r} \right) + f(a, u) = 0, \quad (30)$$

According to the phase-portrait analysis of Eq. (30) [15,16] there are two types of current distributions: filaments in the center of the domain and annular current layers attached to the boundary. With increase of the total current a ‘‘hot’’ central filament (i.e., a filament with high current density in the center) expands over the domain and becomes a ‘‘cold’’ (i.e., low current) annulus attached to the boundary. In a similar way a cold central filament experiences transformation into a hot annulus with decrease of total current. As the condition  $a_0|_{\partial G} = \text{const}$  is met, we conclude that all filamentary and annular states described above are unstable against translation, which breaks the radial symmetry.

On the basis of our analytical considerations we conjecture that all current distributions that have a maximum in the interior of the domain are unstable against translation regardless of the condition  $a_0|_{\partial G} = \text{const}$ . To check this hypothesis we have performed numerical simulations for the model Eqs. (2),(4) for rectangular domains in the current-driven regime [ $R \rightarrow \infty, U_0 \rightarrow \infty, j_0 \equiv U_0/(RS) = \text{const}$ ], which, obviously, corresponds to the case of strong global coupling. Figure 6 shows the time evolution of a center filament in a square domain. The initial configuration corresponds to the stationary solution; the condition  $a_0|_{\partial G} = \text{const}$  is slightly violated. This stationary solution remains stable when perturbations orthogonal to the translation mode are introduced into the numerical simulation (therefore  $\lambda_3 < 0$ ). However, the central filament becomes unstable for random perturbations of arbitrarily small amplitude when the condition of orthogonality is not met ( $\lambda_2 > 0$ ). This instability results in the eventual

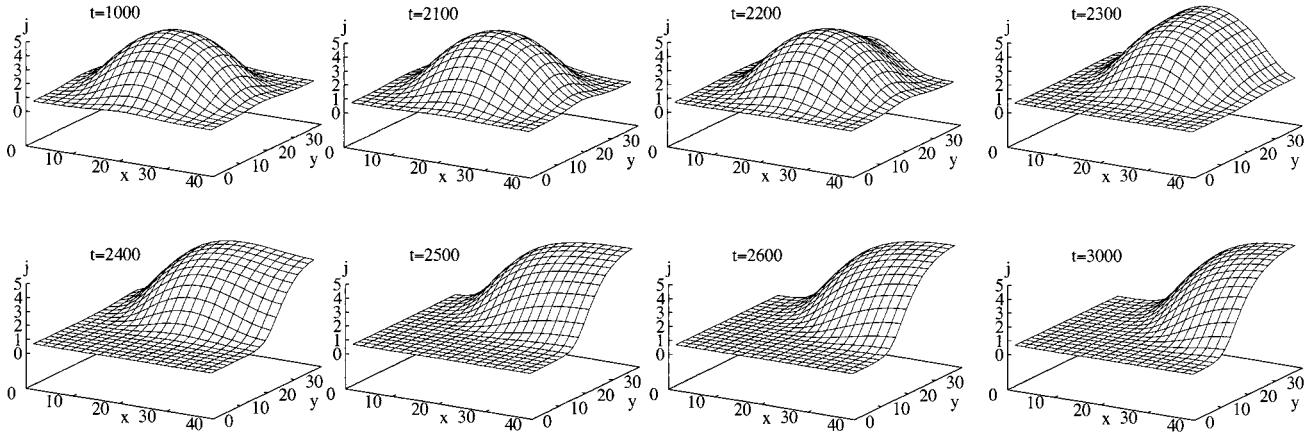


FIG. 6. Instability of a central filament in a square domain. The temporal evolution of the current density  $j(x,y)$  is shown for the following dimensionless numerical parameters:  $j_0 \equiv U_0/(RS) = 1.94$ ,  $C^{-1} = 0.035$ ,  $T = 0.05$ ,  $\tau_a = l_a = 1$ ,  $L = 40$ ,  $L_{cr} = 11.5$ , where  $L_{cr} \equiv \pi l_a (\partial f / \partial a)^{-1/2}$  is the minimum system size necessary for filament formation.

formation of a corner filament, which has its maximum at the boundary. For other parameters the transient process may also lead to an edge current layer. Hot and cold corner filaments and plane edge current layers parallel to the boundary (Fig. 7) are the only structures that arise from random initial conditions in the regime of strong global coupling and represent stable steady states for rectangular domains. Since  $\lambda_1 > 0, \lambda_2 < 0$  their stability depends on the sign of their differential conductance; stability requires  $\sigma_d < 0$ .

Current-voltage characteristics for domains of two different sizes are presented in Fig. 8. Generally, with increasing current the differential conductance changes sign when the filament wall reaches the boundary of the domain: starting from this point the main contribution to the differential conductance is given not by the shift of the filament wall [the second term in Eq. (21)] but by the change of current density in the homogeneous part of the current distribution [the first term in Eq. (21)]. Therefore the differential conductance becomes positive. For edge current layers such a transition occurs for sufficiently thin hot and cold layers. For hot corner filaments the bottom point of the characteristic where the differential conductance changes sign corresponds to a sufficiently small filament; the change at the top of the characteristic takes place when the filament has expanded such that the filament boundary reaches the adjacent corners of the domain [at this point a hot filament covers approximately three-fourth ( $\approx \pi/4$ ) of the domain area]. For cold corner filaments the top and bottom points are interchanged. Sweeping up and down the current-voltage characteristic (Fig. 8) in the current-controlled regime one observes multistability and

multiple hysteresis cycles between edge current layer and corner filaments. The particular scenario of the transitions essentially depends on the ratio  $L/L_{cr}$ .

Our overall conclusion is that a boundary attracts filaments from the interior of the domain. However, the growth increment of the unstable mode decreases with increasing system size. Since therefore in sufficiently large domains a filament in the interior of the domain has nearly neutral stability it may be pinned by a small embedded inhomogeneity of the semiconductor structure. To study the competition between the attracting boundary and pinning at inhomogeneities we have performed the following numerical simulations. Inhomogeneities sensitively influence the transport parameter  $T$  (in the HHED, e.g., this parameter corresponds to a tunneling rate). We assume that  $T$  becomes a function of space, and  $T(x,y)$  has a localized peak of amplitude  $\delta T$  in the center of the square domain. Then for a sufficiently large value of  $\delta T$  the central filament becomes stabilized; i.e., it is pinned at the inhomogeneity. Figure 9 shows the stability in the  $(\delta T, L)$  diagram: the minimum amplitude  $\delta T/T$  of the seed inhomogeneity that is necessary to stabilize a central filament decreases approximately exponentially with the system size  $L$ . This results from the asymptotically exponential decrease of the eigenvalue  $\lambda_2(L)$  of the central filament. Thus, in large domains seed inhomogeneities dominate over boundary effects.

## V. CONCLUSIONS

In bistable semiconductor systems on two-dimensional spatial domains with convex passive boundary (Neumann boundary condition) any stationary nonuniform current den-

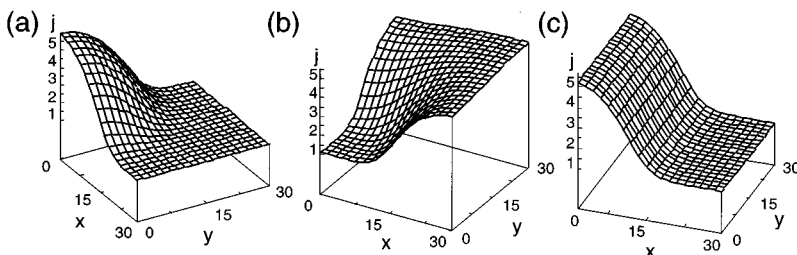


FIG. 7. Stable filament configurations on a square domain: (a) hot and (b) cold corner filament, (c) edge current layer. The values of the average current  $j_0 = U_0/(RS)$  are 1.5, 3.5, 2.0, respectively;  $L = 30$ , other numerical parameters as in Fig. 6.

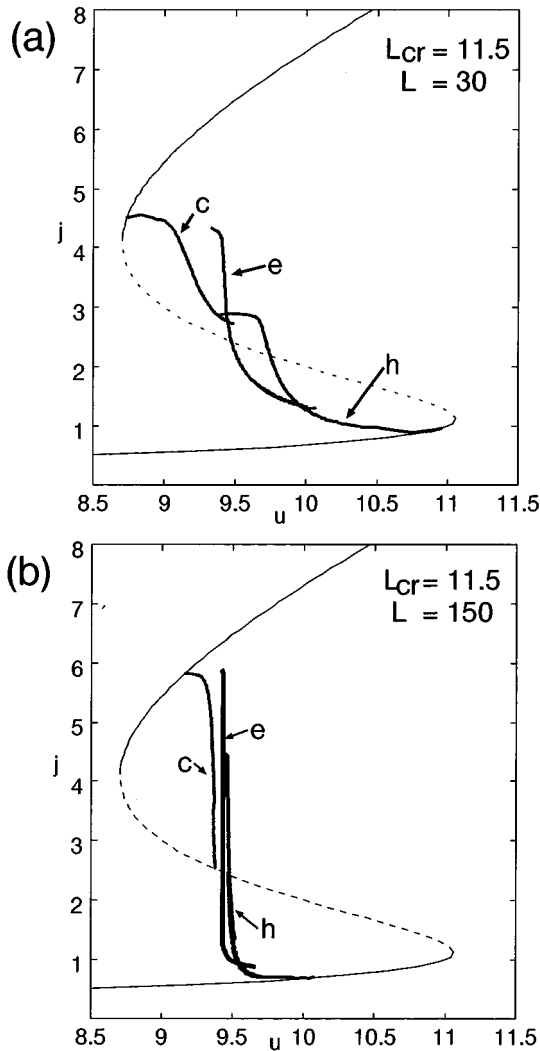


FIG. 8. Current-voltage characteristics for (a) small ( $L=30 \approx 3L_{cr}$ ) and (b) large ( $L=150 \approx 13L_{cr}$ ) square domains. The thin line represents homogeneous states, the thick lines depict the spatially averaged current density of inhomogeneous steady states. Curves  $h, c, e$  correspond to a hot corner filament, a cold corner filament, and an edge current layer, respectively. These branches are stable only in the regime of strong global coupling. Numerical parameters as in Fig. 6.

sity distribution has at least one unstable mode  $\lambda_1 > 0$  when the system is operated in the voltage-driven regime. If the second eigenvalue is negative ( $\lambda_2 < 0$ ) such a distribution can be stabilized by global coupling provided by the external circuit if the stability criteria (28),(29) are satisfied. For filaments with negative differential conductance stability can be

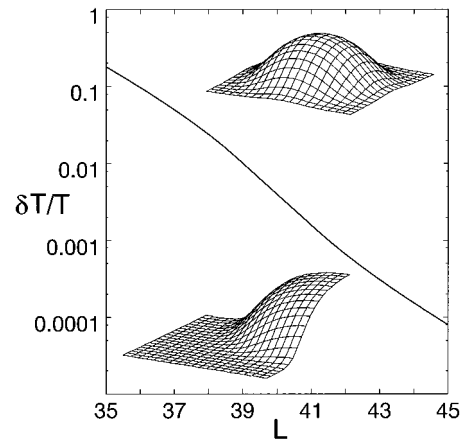


FIG. 9. Effect of structural imperfections on filament stability. The two different regimes are shown in the diagram of the relative amplitude  $\delta T/T$  of seed inhomogeneities vs the system size  $L$ . Upper regime: stable central filament is pinned by a seed inhomogeneity; lower regime: attractive influence of boundary dominates. Other numerical parameters as in Fig. 6.

achieved with a passive ( $R > 0$ ) heavily loaded external circuit. Filaments with positive differential conductance  $\sigma_d$  can be stabilized only by an active external circuit with negative resistance  $R < 0$  when  $\sigma_d > \sigma_u$ . If  $\sigma_d > \sigma_u$ , stabilization of filaments with positive differential conductance requires also a negative total differential capacitance of the device and external circuit  $C = C_{int} + C_{ext} < 0$ . We have proved analytically that  $\lambda_2 > 0$  holds for current distributions that have a maximum in the interior of the spatial domain and a constant value at its boundary. Such distributions, corresponding to central current filaments, remain unstable against translation even if the conditions (28),(29) are satisfied. Our numerical simulations suggest that the condition of constant boundary value may even be relaxed and that Neumann boundaries generally attract current filaments. This is in agreement with numerical results obtained for other reaction-diffusion systems [31]. In structurally imperfect systems seed inhomogeneities tend to pin current filaments in the center; thus there is competition between attractive inhomogeneities and the boundary. In large systems imperfections dominate over boundary effects: the amplitude of the inhomogeneity that is sufficient for pinning current filaments decreases exponentially with increasing transverse dimension of the system.

#### ACKNOWLEDGMENTS

P.R. acknowledges financial support from the Alexander von Humboldt Foundation. Part of this work was supported by the Deutsche Forschungsgemeinschaft.

- [1] *Nonlinear Dynamics and Pattern Formation in Semiconductors and Devices*, edited by F. J. Niedernostheide (Springer, Berlin, 1995).  
 [2] A. Turing, *Philos. Trans. R. Soc. London, Ser. B* **237**, 37 (1952).

- [3] G. Nicolis and I. Prigogine, *Self-Organization in Non-Equilibrium Systems* (Wiley, New York, 1977).  
 [4] B. S. Kerner and V. V. Osipov, *Autosolitons* (Kluwer, Dordrecht, 1994).  
 [5] H.-G. Purwins, C. Radehaus, T. Dirksmeyer, R. Dohmen, R.

- Schmeling, and H. Willebrand, Phys. Lett. A **136**, 480 (1989).
- [6] A. S. Mikhailov, *Foundation of Synergetics I* (Springer, Berlin, 1994).
- [7] *Self-Organization in Activator-Inhibitor-Systems: Semiconductors, Gas-Discharge and Chemical Active Media*, edited by H. Engel, F. J. Niedernostheide, H.-G. Purwins, and E. Schöll (Wissenschaft und Technik Verlag, Berlin, 1996).
- [8] B. K. Ridley, Proc. Phys. Soc. London **82**, 954 (1963).
- [9] A. F. Volkov and Sh. M. Kogan, Zh. Eksp. Teor. Fiz. **52**, 1647 (1967) [Sov. Phys. JETP **25**, 1095 (1967)].
- [10] A. F. Volkov and Sh. M. Kogan, Usp. Phys. Nauk **96**, 633 (1968) [Sov. Phys. Usp. **11**, 881 (1969)].
- [11] F. G. Bass, V. S. Bochkov, and Yu. Gurevich, Zh. Eksp. Teor. Phys. **58**, 1814 (1970) [Sov. Phys. JETP **31**, 972 (1970)].
- [12] I. V. Varlamov and V. V. Osipov, Fiz. Tekh. Poluprovodn. **3**, 950 (1969) [Sov. Phys. Semicond. **3**, 803 (1970)].
- [13] I. V. Varlamov, V. V. Osipov, and E. A. Poltoratsky, Fiz. Tekh. Poluprovodn. **3**, 1162 (1969) [Sov. Phys. Semicond. **3**, 978 (1970)].
- [14] V. V. Osipov and V. A. Kholodnov, Fiz. Tekh. Poluprovodn. **4**, 1216 (1970) [Sov. Phys. Semicond. **4**, 1033 (1971)].
- [15] V. L. Bonch-Bruevich, I. P. Zvyagin, and A. G. Mironov, *Domain Electrical Instabilities in Semiconductors* (Consultant Bureau, New York, 1975).
- [16] E. Schöll, *Nonequilibrium Phase Transitions in Semiconductors* (Springer, Berlin, 1987).
- [17] D. Jäger, H. Baumann, and R. Symanczyk, Phys. Lett. A **117**, 141 (1986).
- [18] F.-J. Niedernostheide, M. Arps, R. Dohmen, H. Willebrand, and H.-G. Purwins, Phys. Status Solidi B **172**, 249 (1992).
- [19] A. V. Gorbatyuk and P. B. Rodin, Solid-State Electron. **35**, 1359 (1992).
- [20] A. V. Gorbatyuk and P. B. Rodin, Radiotekhnika i Elektronika **5**, 910 (1992) [Sov. J. Commun. Technol. Electron. **37**, 97 (1992)].
- [21] M. Shaw, V. Mitin, E. Schöll, and H. Grubin, *The Physics of Instabilities in Solid State Electron Devices* (Plenum Press, New York, 1992).
- [22] F.-J. Niedernostheide, B. S. Kerner, and H.-G. Purwins, Phys. Rev. B **46**, 7559 (1992).
- [23] E. Schöll and D. Drasdo, Z. Phys. B **81**, 183 (1990).
- [24] R. E. Kunz and E. Schöll, Z. Phys. B **89**, 289 (1992).
- [25] A. Wacker and E. Schöll, Z. Phys. B **93**, 431 (1994).
- [26] S. Bose, A. Wacker, and E. Schöll, Phys. Lett. A **195**, 144 (1994).
- [27] F.-J. Niedernostheide, H.-J. Schulze, S. Bose, A. Wacker, and E. Schöll, Phys. Rev. E **54**, 1253 (1996).
- [28] L. Schimansky-Geier, Ch. Zülicke, and E. Schöll, Z. Phys. B **84**, 433 (1991).
- [29] M. Gaa, R. E. Kunz, and E. Schöll, Phys. Rev. B **53**, 15 971 (1996).
- [30] K. Kunihiro, M. Gaa, and E. Schöll, Phys. Rev. B **55**, 2207 (1997).
- [31] F.-J. Niedernostheide, M. Or-Guil, M. Kleinkes, and H.-G. Purwins, Phys. Rev. E **55**, 4107 (1997).
- [32] M. Meixner, A. De Wit, S. Bose, and E. Schöll, Phys. Rev. E **55**, 6690 (1997).
- [33] A. Wacker and E. Schöll, J. Appl. Phys. **78**, 7352 (1995).
- [34] Yu. M. Svirezhev, *Nonlinear Waves, Dissipative Structures and Catastrophies in Ecology* (Nauka, Moscow, 1987) (in Russian).
- [35] M. Reed and B. Simon, *Methods of Modern Mathematical Physics, Vol.4.: Analysis of Operators* (Academic Press, New York, London, 1972).
- [36] A. Gorbatyuk and P. Rodin, Z. Phys. B **104**, 45 (1997).
- [37] W. R. Derrick, *Introductory Complex Analysis and Applications* (Academic Press, New York, London, 1972).
- [38] A. D. Martin, M. L. Lerch, P. E. Simmonds, and L. Eaves, Appl. Phys. Lett. **64**, 1248 (1994).